J Therm Anal Calorim (2017) 129:1233–1241
DOI 10.1007/s10973-017-6174-y

Thermogravimetric analysis of the biomass pyrolysis with copper slag as heat carrier

Pyrolysis characteristics and kinetics

Zongliang Zuo[1] · Qingbo Yu[1] · Huaqing Xie[1] · Wenjun Duan[1] · Sihong Liu[1] · Qin Qin[1]

Received: 9 October 2016 / Accepted: 6 February 2017 / Published online: 23 February 2017

Abstract Thermo gravimetric analysis experiments were carried out on pyrolysis of three kinds of biomasses by temperature programming method. Employed by thermogravimetric analyzer, the effects of the type of biomass and the ratio of copper slag addition on pyrolysis were studied. Biomass pyrolysis process can be divided into four stages, dehydration, pre-pyrolysis, pyrolysis and carbonization. The experimental yields in this paper were modeled by CH_4, C_2H_6, C_3H_8, C_2H_4 and C_3H_6, considering first-order primary reaction and reactions of alkanes and alkenes. Copper slag is beneficial for biomass pyrolysis. With Coats–Redfern method, nonlinear regression of biomass catalytic pyrolysis showed that reaction mechanism of pyrolysis process confirms well with shrinking core model (A3). The kinetic parameters and equations were also calculated. Copper slag promotes both the primary reactions of biomass pyrolysis and the Cracking reactions of alkanes and alkenes, but it cannot decrease the activation energy effectively.

Keywords Copper slag · Pyrolysis · Biomass · Thermodynamic analysis

Introduction

Biomass is expected to be one of the major global primary energy sources. The future, modern, efficient and sustainable uses of biomass are considered much promising and even inescapable in the future [1]. For the efficient utilization of biomass energy, thermochemical conversion technology has drawn much attention of scholars [2–4]. Biomass pyrolysis is a highly endothermic chemical reaction and consumes additional energy sources. Tar vapor is a by-product generated during pyrolysis process, and it contains large amounts of carbon and energy [5]. In the pyrolysis process, tar material may cause operational problems such as pipe blocking, condensation and tar aerosol formation [6]. The treatment of tar is the key to solve the problems above for the biomass pyrolysis gasification technology. At present, the most economic and effective method is conversion by pyrolysis catalytic. Catalytic can not only promote the crack of tar but also improve the composition of gas products. At high temperature, the tar generated by biomass can crack deeply at the surface of catalytic. Promoted by catalytic, micro molecule hydrocarbon compounds take part in the Reforming reaction and react with H_2O and CO_2 [7].

The types of catalytic fall into two major categories, natural ore (dolomite [8, 9], olivine [10], clay etc.) and synthetic catalyst (alkalis catalyst [11], nickel-based catalyst [12] and composite-type catalyst [13]). Natural ore catalyst is more inexpensive than synthetic catalyst. And as natural ore catalyst, olivine is abundant and it has good performance of abrasive resistance at high temperature, which can be applied to fluidized bed. Swierezynski [14] used nickel-based olivine as catalyst to improve the process of steam biomass gasification in a fluidized bed. Its catalytic performances are confirmed in the steam reforming of methane and toluene as a tar model compound. Xie [15] used nickel-based catalyst to study the steam reforming of tar in a hot coke oven for hydrogen production. In experiments, CaO was added to improve the catalyst adsorption characteristics. Nordgreen [16] studied the catalyst

✉ Qingbo Yu
yuqb@smm.neu.edu.cn

[1] School of Metallurgy, Northeastern University, P.O. Box 345, No 11, Lane 3, Wenhua Road, Heping District, Shenyang 110819, Liaoning, People's Republic of China

characteristics of metallic iron on the crack of tar in fluidized bed gasification.

Zhao and Li [17, 18] studied the properties of sawdust gasification by experiments. In Zhao's experiment, the thermal stability of the MSW was analyzed by thermogravimetric analysis, and effects of BF slag on the gas products were investigated at 600–900 °C [17]. And in Li's experiment, the catalytic activity was evaluated by analyzing its phase composition [18]. Pyrolysis process in this research is the primary reaction of gasification process. And the catalyst function of copper slag gasification is similar to pyrolysis process with copper slag as heat carrier and catalyst. The crack reactions are promoted, which would take place in both gasification and pyrolysis process. Promoted by copper slag, the crack of tar increased the fractions of H_2 and CO_2 in gas production. Analyzed by XRD patterns, the activation components in copper slag were Fe_2O_3 and Fe_3O_4.

The use of biomass pyrolysis technology can realize the efficient recovery of waste heat from copper slag. With copper slag as heat carrier and catalytic, pyrolysis kinetics of three typical biomasses were studied in this paper. Thermogravimetric (TG) analysis has been widely used over the years to investigate the thermal events during pyrolysis of biomass, and it provides quantitative results regarding the mass loss of a sample as a function under isothermal or non-isothermal conditions [19–22].

The pyrolysis process of the mixture of copper slag and biomass was discussed by TG analysis with temperature programming method. Gas products were measured and investigated in control experiment device. By Coats–Redfern method, the kinetic parameters and equations were also calculated, respectively, for the biomass pyrolysis with copper slag as heat carrier.

Experimental

Materials

The copper slag samples were from flash smelting furnace by water quenching treatment. Before experiments, copper slag samples were crushed to the size smaller than 250 μm. The composition of copper slag is shown in Table 1. From Table 1, the element content of Fe (MFe, Fe^{2+} and Fe^{3+}) reaches to 44.08% in copper slag. And FeO, SiO_2 and Fe_3O_4 are the main compositions in copper slag. Identified by X-ray diffractometer (Shimadzu, XRD-7000), the phases in raw materials are fayalite (Fe_2SiO_4) and magnetic (Fe_3O_4), as shown in Fig. 1.

The biomass materials are corncob, pine sawdust and straw from Liaoning Province of China (abbreviated as CN, PE, and SW, respectively). After drying in vacuum drying oven at 353 K for 12 h, the samples were sieved to 150 μm. The analytical data (proximate analysis, components analysis and ultimate analysis) for the biomass samples are shown in Table 2. From the analysis data, PE has the highest content of volatile and CN has the highest content of fixed carbon. It can be seen that hemicellulose, cellulose and lignin are the three main components of the biomass. And the contents of cellulose, lignin for PE are highest. By ultimate analysis, the content of carbon in PE is higher than CN and PE.

Apparatus and methods

A NETZSCH STA409PC thermogravimetric analyzer was employed. Biomass and copper slag were mixed thoroughly and then placed in a high-purity aluminum crucible. The protective gas was Ar and its flow rate was 30 mL min^{-1}, controlled by flow meters. In each experiment, about 10 mg of the samples were heated from 298 to 1173 K at a heating rate of 10, 20 and 40 K min^{-1}, respectively.

And at the same heating rate and atmosphere, samples were put into a pipe-typed furnace. Pyrolysis reactions of biomass took place in furnace, and the gas products were measured by gas analysis meter. The experimental conditions are shown in Table 3. The mass ratio of biomass/copper slag was abbreviated as *B*/*S*.

Experimental results and discussion

Biomass pyrolysis characteristics

Mass loss curve (TG) and mass loss rate curve (DTG) of biomass (PE as an example) pyrolysis are shown in Fig. 2. And the composition variation of biomass pyrolysis gas is shown in Fig. 3. CO_2, CO, CH_4 and H_2 are the main components in biomass pyrolysis gas. Figure 4 is the FTIR spectra of three types of biomass. Figure 5 is FTIR spectra of fixed carbon pyrolysis from CN, PE and SW. According to Figs. 4 and 5, pyrolysis of biomass is accompanied with the crack of bond (C=O, C–O) and the divorce of micromolecule (–OH, CH_2, –CN, –CH, $–NH_2$). Based on the analysis of TG, DTG and gas composition during heating process, biomass pyrolysis process can be divided into four stages.

1. Dehydration (<393 K). During this stage, free water breaks away from biomass without reactions taking place.
2. Pre-pyrolysis (393–453 K). Without mass loss, the temperature of biomass increases gradually. The structure rearranges and reconciliation polyethylene reaction takes place inside the biomass.

Table 1 Compositions of copper slag, mass%

FeO	Fe_3O_4	CaO	Al_2O_3	MFe	SiO_2	Cu	MgO	S	Zn	others
37.50	18.90	0.23	0.98	1.24	31.99	0.74	0.42	0.39	2.78	4.87

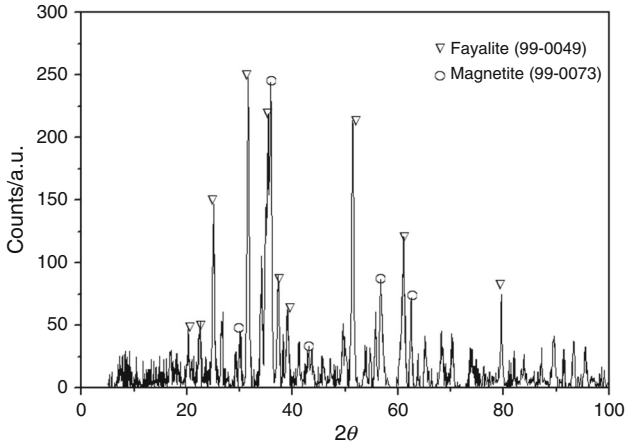

Fig. 1 Picture of X-ray diffraction spectrogram of copper slag

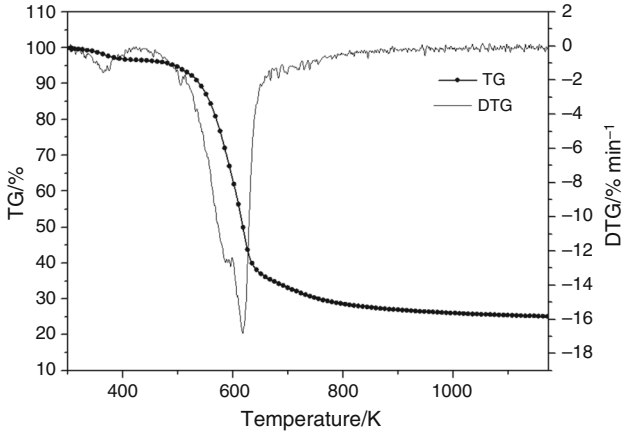

Fig. 2 Curves of biomass pyrolysis characteristics (PE)

Table 2 Properties of three biomass materials

Samples	CN	PE	SW
Proximate analysis/mass%			
Moisture	6.07	3.81	6.84
Volatiles matter	73.54	79.01	67.90
Ash	3.43	2.17	9.36
Fixed carbon	16.96	15.01	15.90
Components analysis/mass%			
NDF	17.93	10.99	32.02
Hemicellulose	18.74	5.90	18.38
Cellulose	53.69	58.88	39.68
Lignin	8.75	23.42	7.38
Ultimate analysis/mass%			
Nitrogen	1.65	0.15	0.61
Carbon	41.34	48.28	45.16
Hydrogen	5.769	6.17	5.928
Sulfur	0.125	0.082	0.069

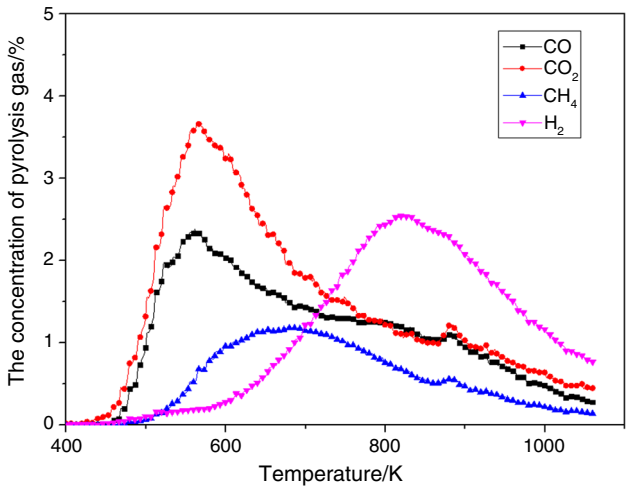

Fig. 3 Composition variation of biomass pyrolysis gas

3. Pyrolysis (453–773 K). Cellulose in biomass depolymerizes to monomer. And then, pyrolysis products are generated by free radical reaction and rearrangement

Table 3 Experimental conditions

Biomass type	B/S	Heating rate/K min^{-1}	Start temperature/K^{-1}	Final temperature/K^{-1}	Atmosphere
CN	1:0	20	308	1173	Ar
PE	1:0.5				
SW	1:1				
	1:2				

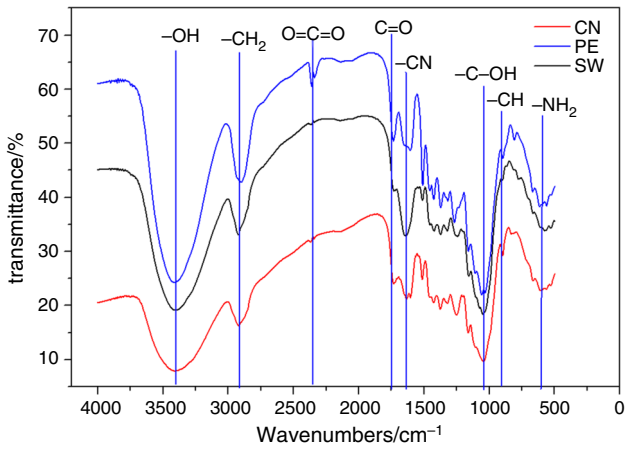

Fig. 4 FTIR spectra of three types of biomass

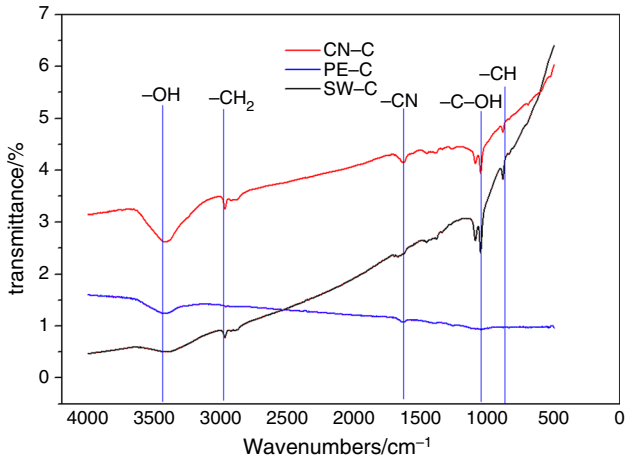

Fig. 5 FTIR spectra of fixed carbon by CN, PE and SW

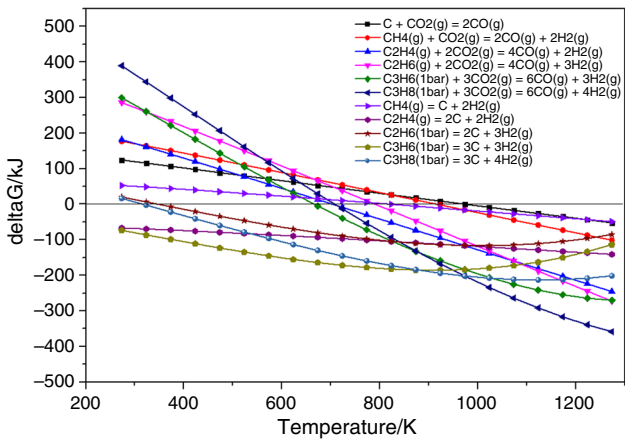

Fig. 6 Gibbs free energy variation of gas conversion reaction versus temperature

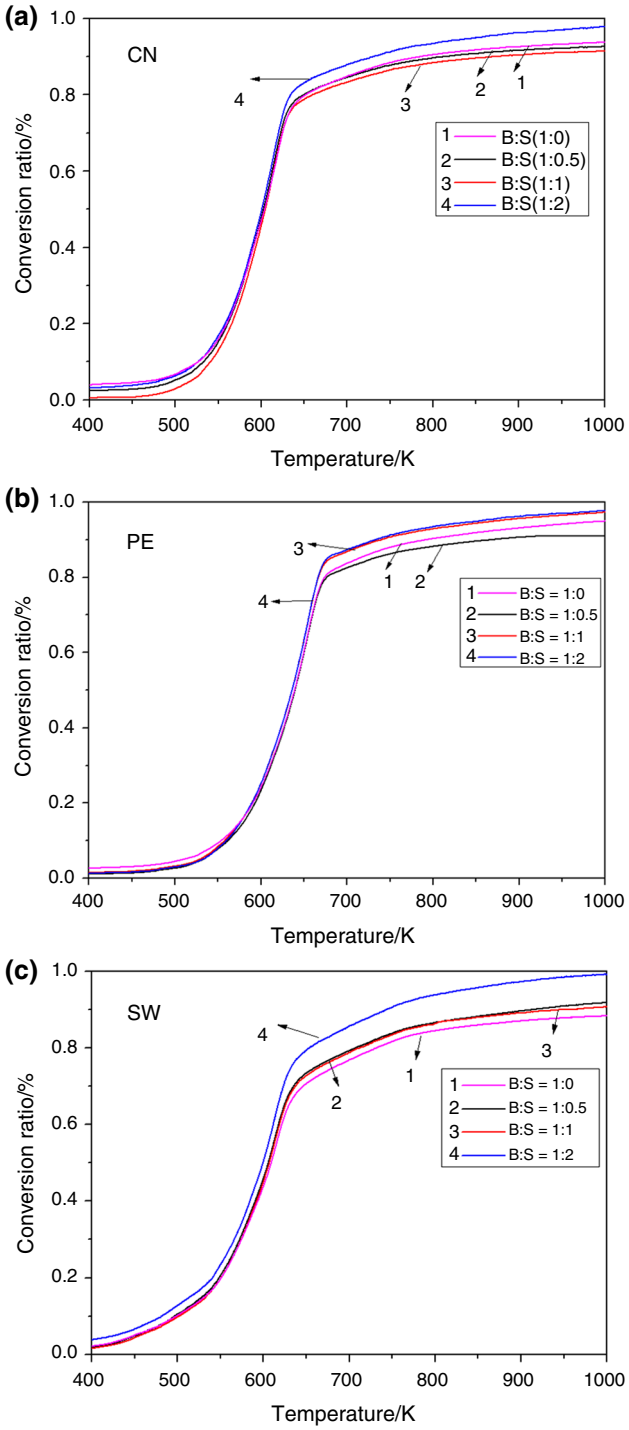

Fig. 7 Conversation of three kinds of biomasses at different ratio of copper slag

reactions. Carbon bond fractures in hemicellulose and cellulose are accompanied with the production of CO and CO_2. With the increase in temperature, the concentration of CO and CO_2 reaches maximum at 823 K. When the concentrations of CO and CO_2 begin to decrease, the concentrations of CH_4 and H_2 begin to increase slowly. Reactions about breaks of C-H also take place in this stage.

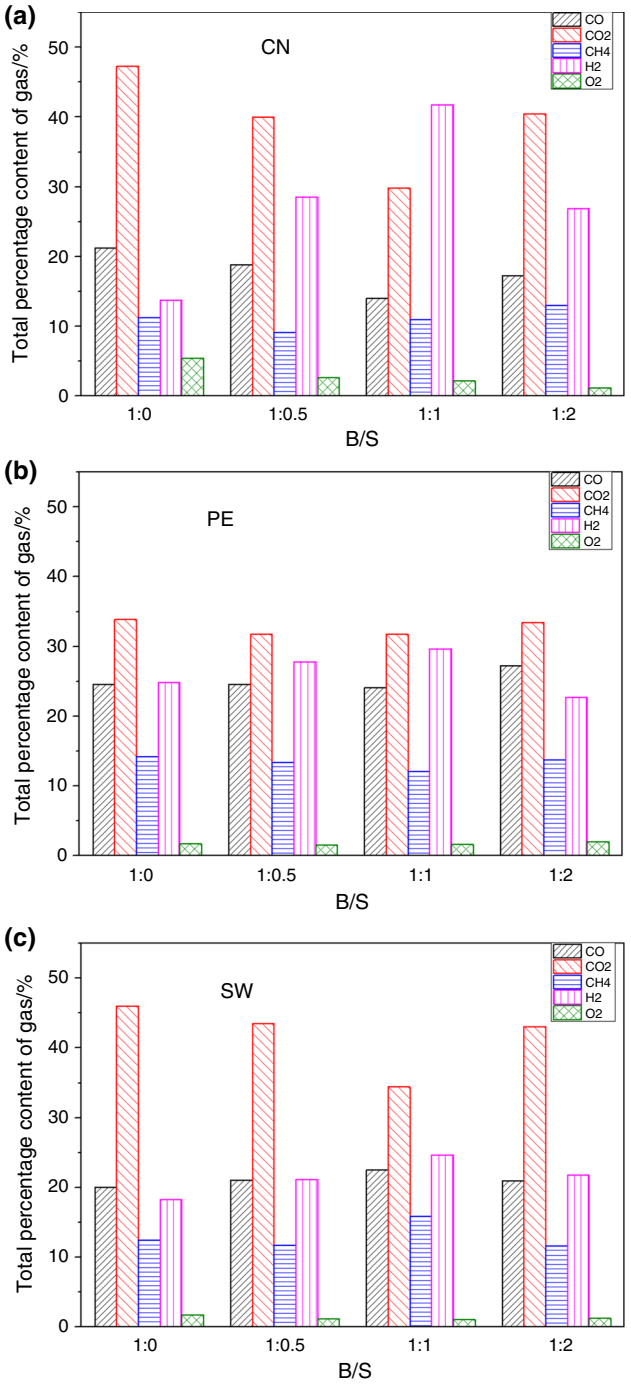

Fig. 8 Composition of biomass pyrolysis gas change curves versus ratio of copper slag

4. Carbonization (>773 K). Mass of biomass decrease slowly accompanied with polymerization reactions and carbonization reactions. Fixed carbon and biomass ash are generated in this stage. And the reduction in copper slag takes place above 1100 K, which would be eliminated in this stage [23].

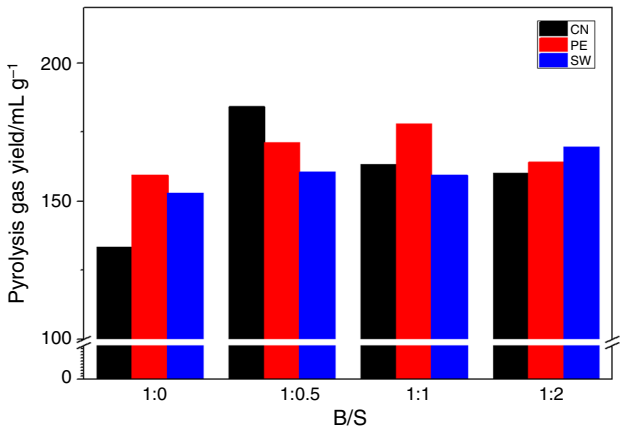

Fig. 9 Pyrolysis gas yield with the change of ratio of copper slag

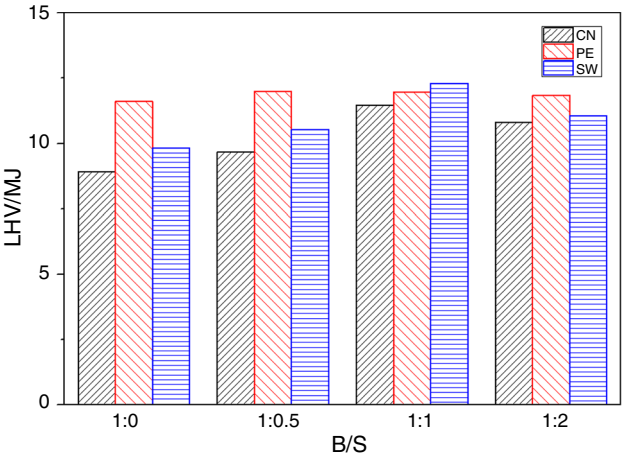

Fig. 10 Pyrolysis gas LHV with the change of ratio of copper slag

Thermal analysis for gas conversion reactions for biomass pyrolysis

Copper slag can act as catalyst for biomass gasification. In copper slag, Fe_3O_4 and Fe_2O_3 are the activation components [17, 18]. Condensable volatiles can decompose under the action of the catalysis of copper slag. Coupled chemical reactions in pyrolysis mainly include gas shift reactions. Gas shift reactions include Boudouard reaction (Eq. 1), Reforming reaction (Eq. 2) and Cracking reaction (Eq. 3). In Boudouard reaction, the generation of CO leads to mass loss of sample. The reagent and product participated in the reactions were all gas. Thus, Reforming reaction does not change the mass of sample. In Cracking reaction, the generation of fixed carbon leads to the mass increment.

The Gibbs free energy variation of gas conversion reactions is shown in Fig. 6. For the complexity of pyrolysis gas composition, it is unrealistic to confirm every reaction in pyrolysis process. Alkanes and alkenes participated in

Reforming reaction and Cracking reaction. Thus, the experimental yields in our work are modeled by CH_4, C_2H_6, C_3H_8, C_2H_4 and C_3H_6, considering first-order primary reaction and reactions of alkanes and alkenes [24]. From Fig. 6, the Gibbs free energy of three kinds of reactions progressively decreased with the increase in temperature. Boudouard reaction can take place spontaneously above 970 K. In pyrolysis temperature interval (453–773 K), Gibbs free energy of Cracking reactions are lower than Reforming reactions, which means that it is easier for Cracking reactions to take place in this condition. When the temperature is lower than 900 K, Cracking reactions of C_2H_6, C_3H_8, C_2H_4 and C_3H_6 can take place spontaneously, but Boudouard reaction, Reforming and Cracking reactions of CH_4 cannot take place spontaneously.

$$\text{Boudouard reaction:} \quad C + CO_2(g) = 2CO(g) \tag{1}$$

$$\text{Reforming reaction:} \quad C_mH_n(g) + mCO_2(g) = 2mCO(g) + \frac{n}{2}H_2(g) \tag{2}$$

$$\text{Cracking reaction:} \quad C_mH_n(g) = mC + \frac{n}{2}H_2(g) \tag{3}$$

Effects of copper slag on biomass pyrolysis characteristics

Figure 7 is the conversation of three kinds of biomasses at different ratios of copper slag. When the ratio of *B*/*S* is 1:2, the conversion ratio of copper slag on biomass can improve inordinately. The effect rule for copper slag on biomass pyrolysis characteristics is different. When *B*/*S* is 1:0.5 and 1:1, the conversion ratio does not change obviously and inordinately. There are two speculations based on the mass change of reactions for the phenomenon above. On the one hand, copper slag can promote primary reactions of biomass pyrolysis and Cracking reactions for pyrolysis gas products. On the other hand, copper slag can promote Boudouard reaction and Cracking reactions for pyrolysis gas product. In other words, the promote effects of copper slag on mass increase reactions and decrease reactions exist simultaneously. In order to identify the speculations above, the gas products of pyrolysis were studied below.

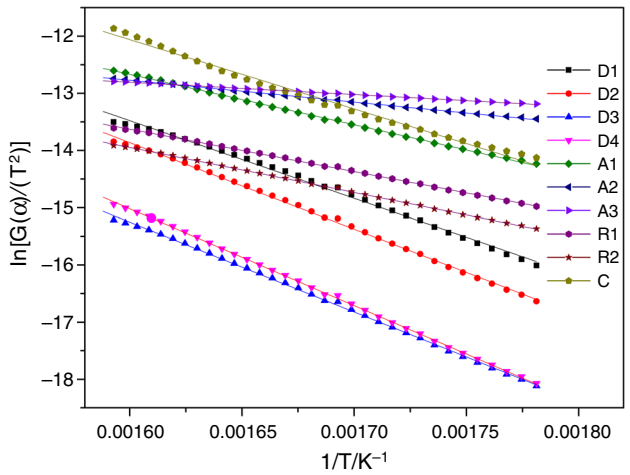

Fig. 11 Linear regression curves of different models (CN)

Figure 8 is the composition of biomass pyrolysis gas with the change of the mass ratio of copper slag. The content of pyrolysis gas changes with the type of biomass. The content of CO_2 in pyrolysis is higher than any other gas products. The content of CO_2 from CN is the highest and reaches to 48%. As shown in Fig. 8, the addition of copper slag can increase H_2 yield and decrease CO yield. And the effect of copper slag on CN pyrolysis is more obvious than PE and SW.

Figures 9 and 10 are the gas yield and gas LHV with the change of ratio of copper slag. As shown in Fig. 9, the addition of copper slag increased the production of pyrolysis gas. This means that copper slag promotes pyrolysis primary reactions. From Fig. 10, copper slag improved the LHV of pyrolysis gas. And when *B*/*S* is 1:1, the LHV of three kinds of biomasses are highest.

The catalyst function of fayalite and magnetite in copper slag is similar to dolomite [25, 26]. However, the specific surface area of copper slag is lower than dolomite for the lack of porous structure. The catalyst function of copper slag is by its component other than structure. Some primary products of biomass pyrolysis and pyrolysis gas product are electronegative. When they are absorbed on the active site on copper slag, they became unsteady. And Cracking reactions take place in this condition.

Dynamic kinetics of biomass pyrolysis with copper slag

Coats–Redfern method [27] was used to analyze the kinetics characteristics of biomass catalytic pyrolysis, indicated that it can be used by multi-step reactions rather than simple first-order reaction [28]. In this paper, based on Coats–Redfern method, the kinetics of biomass pyrolysis could be described as follows:

$$\frac{d\alpha}{dt} = kf(\alpha) \tag{4}$$

The conversion ratio α, reaction rate k and heating rate β are expressed as follows:

$$\alpha = \frac{m_0 - m_t}{m_0 - m_1} \tag{5}$$

$$k = A\exp\left(-\frac{E}{RT}\right) \tag{6}$$

$$\beta = \frac{dT}{dt} \tag{7}$$

Table 4 Reaction kinetics models

Models	Symbol	Rate equation $f(\alpha)$	Reaction mechanism equation $G(\alpha)$
One-dimension diffusion	D_1	$1/2\alpha$	α^2
Two-dimension diffusion (cylindrical symmetry)	D_2	$[-\ln(1-\alpha)]^{-1}$	$\alpha+(1-\alpha)\ln(1-\alpha)$
Three-dimension diffusion(cylindrical symmetry)	D_3	$(3/2)[(1-\alpha)]^{-1/3}-1]^{-1}$	$1-(2/3)\alpha]-(1-\alpha)^{2/3}$
Three-dimension diffusion (spherical symmetry)	D_4	$(3/2)(1-\alpha)^{2/3}\left[1-(1-\alpha)^{2/3}\right]^{-1}$	$\left[1-(1-\alpha)^{1/3}\right]^2$
Random nucleation ($n=1$)	A_1	$1-\alpha$	$-\ln(1-\alpha)$
Random nucleation ($n=2$)	A_2	$2(1-\alpha)[-\ln(1-\alpha)]^{1/2}$	$[-\ln(1-\alpha)]^{1/2}$
Random nucleation ($n=3$)	A_3	$3(1-\alpha)[-\ln(1-\alpha)]^{2/3}$	$[-\ln(1-\alpha)]^{1/3}$
Shrinking core (cylindrical symmetry)	R_1	$2(1-\alpha)^{1/2}$	$1-(1-\alpha)^{1/2}$
Shrinking core (spherical symmetry)	R_2	$3(1-\alpha)^{2/3}$	$1-(1-\alpha)^{1/3}$
Chemical reaction ($n=2$)	C	$(1-\alpha)^2$	$(1-\alpha)^{-1}-1$

Table 5 Results of pyrolysis dynamics model parameters of the three biomasses

Types of biomass	*B*/*S*	*E*/kJ mol^{-1}	*A*/s	R^2	RSS
CN	1:0	32.398	0.660	0.9987	0.0197
CN	1:0.5	29.547	0.600	0.9987	0.0227
CN	1:1	33.180	1.550	0.9991	0.0171
CN	1:2	31.523	0.918	0.9973	0.0468
PE	1:0	34.010	1.024	0.9940	0.0963
PE	1:0.5	30.798	0.504	0.9962	0.0713
PE	1:1	33.097	0.993	0.9932	0.1132
PE	1:2	31.830	0.664	0.9927	0.1413
SW	1:0	19.531	0.056	0.9956	0.0341
SW	1:0.5	20.408	0.078	0.9952	0.0295
SW	1:1	20.980	0.051	0.9958	0.0325
SW	1:2	20.582	0.067	0.9910	0.0772

Equation (4) can be converted to:

$$\frac{\mathrm{d}\alpha}{f(\alpha)}=\frac{A}{\beta}\exp\left(-\frac{E}{\mathrm{R}T}\right)\mathrm{d}T \tag{8}$$

where α is the conversion ratio, %; m_0, m_1 and m are the sample masses at the start, the end and at time t, respectively, g; k is the chemical reaction rate constant; β is the heating rate, K min^{-1}; $f(\alpha)$ is the mechanism function; A is the pre-exponential factor, min^{-1}; E is the activation energy, kJ mol^{-1}; and R is the universal gas constant, kJ mol^{-1} K^{-1}.

Then by integrating Eq. (8), we can get:

$$G(\alpha)=\int_0^{\alpha}\frac{\mathrm{d}\alpha}{f(\alpha)}=\int_0^{T}\frac{A}{\beta}\exp\left(-\frac{E}{\mathrm{R}T}\right)\mathrm{d}T \tag{9}$$

For convenient, the term of $u=E/\mathrm{R}T$ is introduced [27]:

$$\int_0^{T}\frac{A}{\beta}\exp\left(-\frac{E}{\mathrm{R}T}\right)\mathrm{d}T=-\frac{E}{\mathrm{R}}\int_u^{\infty}e^{-\mathrm{u}}u^{-2}\mathrm{d}u \approx\frac{E}{\mathrm{R}}\left(1-\frac{2}{u}\right)u^2e^{-\mathrm{u}} \tag{10}$$

$$\ln\left[\frac{G(\alpha)}{T^2}\right]\approx\ln\left[\frac{AR}{\beta E}\left(1-\frac{2RT}{E}\right)\right]-\frac{E}{RT} \tag{11}$$

As the term of $2RT/E$ is far less than 1 and can be neglected, Eq. (11) can be simplified as:

$$\ln\left[\frac{G(\alpha)}{T^2}\right]\approx\ln\left(\frac{\mathrm{AR}}{\beta E}\right)-\frac{E}{\mathrm{R}T} \tag{12}$$

The relationship between T and $G(\alpha)/T^2$ in Eq. (12) is transformed into a linear function. As shown in Fig. 11, by linear fitting of 10 mechanism functions in Table 4 [29], the linear correlation coefficient R^2 and regression square sum RSS are obtained. Firstly the relevance results of 10 mechanism functions were compared. The relevance of D3, D4, A1, A2, A3 and R1 was all above 0.99. Then, the sum RSS of six models above were compared. The RSS calculated results of model A3 are lower than others. Based on Arrhenius equation, the pyrolysis reaction of biomass confirms well with shrinking core model (A3). Therefore, the kinetic equation is established as:

$$\frac{\mathrm{d}\alpha}{\mathrm{d}T}=\frac{A_\mathrm{i}}{\beta}\left(-\frac{E_\mathrm{i}}{RT}\right)\left[3(1-\alpha)[-\ln(1-\alpha)]^{2/3}\right] \tag{13}$$

where, E_i and A_i are activation energy and pre-exponential factor in different conditions, respectively. The results of dynamics model parameters are shown in Table 5.

From Table 5, the exit of copper slag did not change pyrolysis dynamic model. And the activation energy did not decrease with the addition of copper slag for three kinds of biomasses. Figure 12 is the pyrolysis process

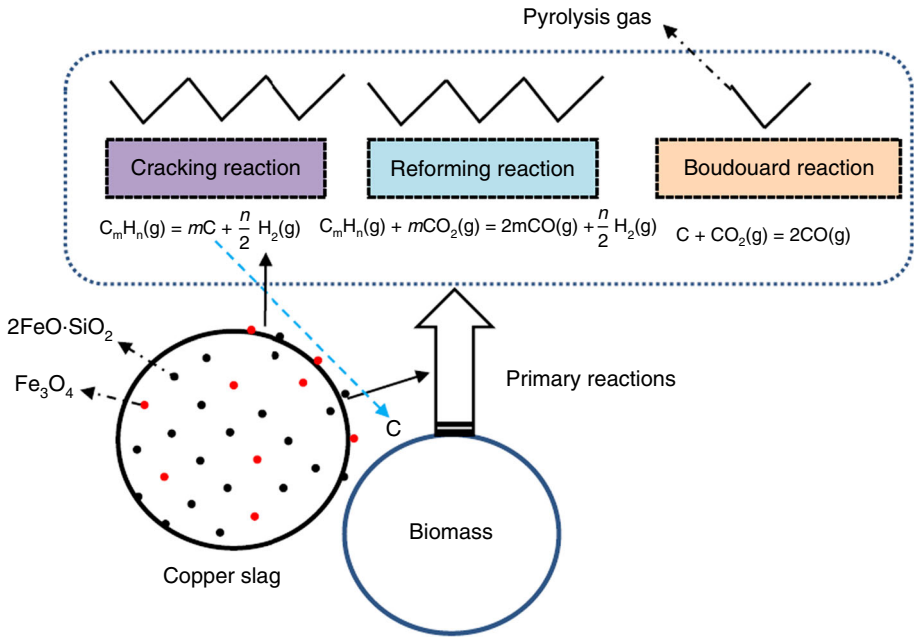

Fig. 12 Pyrolysis process diagram

diagram for biomass with copper slag. As shown in Fig. 12, compared with the experiment results in "Effects of copper slag on biomass pyrolysis characteristics" section, copper slag promotes both the primary reactions of biomass pyrolysis and the Cracking reactions of alkanes and alkenes. In pyrolysis process, C atom is fixed in fixed carbon, which leads to mass increase in the samples. And mass increment makes activation energy does not change obviously. All in all, copper slag is beneficial for biomass pyrolysis and it can increase H_2 production, improve pyrolysis gas composition and increase calorific value, but it cannot decrease the activation energy effectively.

Conclusions

The results obtained from this work indicate that copper slag would be a potential good heat carrier for the pyrolysis of biomass. The following items were concluded:

1. Pyrolysis of biomass is accompanied with the crack of bond (C=O, C–O) and the divorce of micromolecule (–OH, $–CH_2$, –CN, –CH, $–NH_2$). And biomass pyrolysis process can be divided into four stages, dehydration (<393 K), pre-pyrolysis (393–453 K), pyrolysis (453–773 K) and carbonization (>773 K). Coupled chemical reactions in pyrolysis are mainly gas shift reactions. The gas shift reactions are Boudouard reaction, Reforming reaction and Cracking reaction.
2. The addition of copper slag can increase H_2 yield and decrease CO yield. And the effect of copper slag on CN pyrolysis is more obvious than PE and SW. Copper slag is beneficial for biomass pyrolysis, and it can increase H_2 production, improve pyrolysis gas composition and increase calorific value. When *B*/*S* is 1:1, the LHV of three kinds of biomasses are highest.
3. With Coats–Redfern method, nonlinear regression of biomass catalytic pyrolysis showed that reaction mechanism of pyrolysis process confirms well with shrinking core model (A3). Copper slag promotes both the primary reactions of biomass pyrolysis and the Cracking reactions of alkanes and alkenes, but it cannot decrease the activation energy effectively.

Acknowledgements This research was supposed by National Natural Science Foundation of China (51576035), The National Science Foundation for Post-doctoral Scientists of China (No. 2015M571322), The National Key Technologies R&D Program of China (2013BAA03B03), National Natural Science Foundation of China (No.51604077), the Fundamental Research Funds for the Central Universities (N150203006), The Initiative Postdocs Supporting Program (BX201600028).

References

1. Richardson Y, Blin J, Julbe A. A short overview on purification and conditioning of syngas produced by biomass gasification: catalytic strategies, process intensification and new concepts. Prog Energy Combust Sci. 2012;38:765–81.
2. Mohan D, Pittman CU, Steele PH. Pyrolysis of wood biomass for bio-oil: a critical review. Energy Fuels. 2006;20:848–89.
3. Bridgwater AV. Review of fast pyrolysis of biomass and product upgrading. Biomass Bioenergy. 2012;38:68–94.
4. Xie HQ, Yu QB, Qin Q, et al. Study on pyrolysis characteristics and kinetics of biomass and its components. J Renew Sustain Energy. 2013;5:013122.

5. Ziebik A, Lampert K, Szega M. Energy analysis of blast-furnace system operating with the Corex process and CO_2 removal. Energy. 2008;33:199–205.
6. Bakti Cahyono R, Rozhan AN, Yasuda N, Nomura T, Hosokai S, Kashiwaya Y, et al. Integrated coal-pyrolysis tar reforming using steelmaking slag for carbon composite and hydrogen production. Fuel. 2013;109:439–44.
7. Yang XC, Wei YN, Li WJ. Research progress of catalysts for tar cracking. Chem Ind Eng Prog. 2007;26:326–30.
8. Ponzio A, Kalisz S, Blasiak W. Effect of operating conditions on tar and gas composition in high temperature air/steam gasification (HTAG) of plastic containing waste. Fuel Process Technol. 2006;87:223–33.
9. Zhang RQ, Robert CB, Andrew S. Catalytic destruction of tar in biomass derived producer gas. Energy Convers Manag. 2004;45:995–1014.
10. Devi L, Craje M, Thune P, et al. Olivine as tar removal catalyst for biomass gasifier: catalyst characterization. Appl Catal A. 2005;294:68–79.
11. Lizzio AA, Radovic LR. Transient kinetics study of catalytic char gasification in carbon dioxide. Ind Eng Chem Res. 1991;30:1735–44.
12. Tomishige K, Kimura T, Nishikawa J, et al. Promoting effect of the interaction between Ni and CeO_2 on steam gasification of biomass. Catal Commun. 2007;8:161–6.
13. Miyazawa T, Kimura T, Nishikawa J, et al. Catalytic properties of Rh–CeO_2–SiO_2 for synthesis gas production from biomass by catalytic partial oxidation of tar. Sci Technol Adv Mater. 2005;6:604–14.
14. Swierczynski D, Courson C, Bedel L, et al. Characterization of Ni–Fe/MgO/olivine catalyst for fluidized bed steam gasification of biomass. Appl Catal B Environ. 2006;18:4025–32.
15. Xie HQ, Zhang JR, Yu QB, et al. Study on steam reforming of tar in hot coke oven gas for hydrogen production. Energy Fuels. 2016;30:82–90.
16. Nordgreen T, Liliedahl T, Sjostrom K. Metallic iron as a tar breakdown catalyst related to atmospheric fluidised bed gasification of biomass. Fuel. 2006;85:689–94.
17. Zhao LM, Hu JH, Wang H, Qing S, Liu HL, et al. Characteristics of gaseous product from municipal solid waste gasification with hot blast furnace slag. J Nat Gas Chem. 2010;19:403–8.
18. Li JQ, Hu JH, Wang H, Deng SH, Hu W. Experimental study on steam gasification of sawdust with high temperature copper-containing slag. Chin J Process Eng. 2012;12(5):877–81.
19. Wang J, Zhao H. Error evaluation on pyrolysis kinetics of sawdust using iso-conversional methods. J Therm Anal Calorim. 2016;124:1635–40.
20. Sebio-Punal T, Naya S, Lopez-Beceiro J. Thermogravimetric analysis of wood, holocellulose, and lignin from five wood species. J Therm Anal Calorim. 2012;109:1163–7.
21. Oyedun AO, Tee CZ, Hanson S. Thermogravimetric analysis of the pyrolysis characteristics and kinetics of plastics and biomass blends. Fuel Process Technol. 2014;128:471–81.
22. Mu L, Chen JB, Yin HC. Pyrolysis behaviors and kinetics of refining and chemicals wastewater, lignite and their blends through TGA. Bioresour Technol. 2015;180:22–31.
23. Zuo ZL, Yu QB, Wei MQ, Xie HQ, et al. Thermogravimetric study of the reduction of copper slag by biomass. J Therm Anal Calorim. 2016;126:481–91.
24. Pant KK, Kunzru D. Catalytic pyrolysis of methylcyclohexane: kinetics and modeling. Chem Eng J. 1998;70:47–54.
25. Devi L, Craje M, Thune P, et al. Olivine as tar removal catalyst for biomass gasifier: catalyst characterization. Appl Catal A. 2005;294(1):68–79.
26. Devi L, Krzyszt JP, Frans JG, et al. Catalytic decomposition of biomass tars: use of dolomite and untreated olivine. Renew Energy. 2005;30(4):565–87.
27. Coats AW, Redfern JP. Kinetic parameters from thermogravimetric data. Nature. 1964;201:68–9.
28. Lu C, Song W, Lin W. Kinetics of biomass catalytic pyrolysis. Biotechnol Adv. 2009;27:583–7.
29. Li C, Suzuki K. Kinetic analyses of biomass tar pyrolysis using the distributed activation energy model by TG/DTA technique. J Therm Anal Calorim. 2009;98:261–6.